Hypoxia

Dovepress
open access to scientific and medical research

Open Access Full Text Article

ORIGINAL RESEARCH

Resistance of subventricular neural stem cells to chronic hypoxemia despite structural disorganization of the germinal center and impairment of neuronal and oligodendrocyte survival

This article was published in the following Dove Press journal:
Hypoxia
8 June 2015
Number of times this article has been viewed

Xavier d'Anglemont de Tassigny[1,*]
M Salomé Sirerol-Piquer[2,3,*]
Ulises Gómez-Pinedo[4]
Ricardo Pardal[1]
Sonia Bonilla[1]
Vivian Capilla-Gonzalez[2]
Ivette López-López[1]
Francisco Javier De la Torre-Laviana[1]
José Manuel García-Verdugo[2,3]
José López-Barneo[1,3]

[1]Medical Physiology and Biophysics Department, Institute of Biomedicine of Seville (IBiS), Virgen del Rocío University Hospital/CSIC/University of Seville, Seville, Spain; [2]Cavanilles Institute of Biodiversity and Evolutionary Biology, University of Valencia, Valencia, Spain; [3]Network Center of Biomedical Research on Neurodegenerative Diseases (CIBERNED), Spain; [4]Laboratory of Regenerative Medicine, San Carlos Institute of Health Investigation, Madrid, Spain

*These authors contributed equally to this work

Correspondence: José López-Barneo
Institute of Biomedicine of Seville (IBiS), Virgen del Rocío University Hospital, Avenida Manuel Siurot s/n, 41013 Sevilla, Spain
Tel +34 95 592 3001
Fax +34 95 592 3101
Email lbarneo@us.es

José Manuel García-Verdugo
Department of Comparative Neurobiology, Cavanilles Institute of Biodiversity and Evolutionary Biology, University of Valencia, Polígono La Coma s/n, 46980 Paterna, Valencia, Spain
Tel +34 96 354 3769
Fax +34 96 354 3670
Email j.manuel.garcia@uv.es

Abstract: Chronic hypoxemia, as evidenced in de-acclimatized high-altitude residents or in patients with chronic obstructive respiratory disorders, is a common medical condition that can produce serious neurological alterations. However, the pathogenesis of this phenomenon is unknown. We have found that adult rodents exposed for several days/weeks to hypoxia, with an arterial oxygen tension similar to that of chronically hypoxemic patients, manifest a partially irreversible structural disarrangement of the subventricular neurogenic niche (subventricular zone) characterized by displacement of neurons and myelinated axons, flattening of the ependymal cell layer, and thinning of capillary walls. Despite these abnormalities, the number of neuronal and oligodendrocyte progenitors, neuroblasts, and neurosphere-forming cells as well as the proliferative activity in subventricular zone was unchanged. These results suggest that neural stem cells and their undifferentiated progeny are resistant to hypoxia. However, in vivo and in vitro experiments indicate that severe chronic hypoxia decreases the survival of newly generated neurons and oligodendrocytes, with damage of myelin sheaths. These findings help explain the effects of hypoxia on adult neurogenesis and provide new perspectives on brain responsiveness to persistent hypoxemia.

Keywords: neural stem cells, chronic hypoxemia, subventricular germinal niche, ultrastructure, neuronal differentiation, oligodendrocyte survival

Introduction

Chronic hypoxemia is a frequent condition in the human population. Millions of people live or travel at high altitudes and are thus exposed to low atmospheric air pressure and decreased oxygen (O_2) diffusion into the blood.[1,2] In addition, highly prevalent medical disorders such as chronic obstructive pulmonary disease (COPD) can cause severe systemic hypoxia due to reduction of the O_2 exchange capacity between the alveolar gas and the pulmonary capillaries.[3,4] The O_2 tension (pO_2) in some regions of the brain parenchyma can as such reach low values (~10 mmHg or less),[5] which during hypoxemia decrease further to levels that could eventually be deleterious for neuronal function. Indeed, cumulative evidence indicates that COPD patients with marked decrease in blood pO_2 can suffer serious neurological alterations.[4,6–8] In addition, a significant number of high-altitude residents do not acclimatize to hypoxia and develop chronic mountain sickness, presenting sensorimotor alterations, dizziness, and cognitive impairment.[1,9–11]

© 2015 d'Anglemont de Tassigny et al. This work is published by Dove Medical Press Limited, and licensed under Creative Commons Attribution – Non Commercial (unported, v3.0) License. The full terms of the License are available at http://creativecommons.org/licenses/by-nc/3.0/. Non-commercial uses of the work are permitted without any further permission from Dove Medical Press Limited, provided the work is properly attributed. Permissions beyond the scope of the License are administered by Dove Medical Press Limited. Information on how to request permission may be found at: http://www.dovepress.com/permissions.php

Despite its clinical relevance in humans, the pathogenesis of brain dysfunction induced by chronic hypoxemia is poorly known. In particular, the impact of sustained low blood pO_2 on areas of the adult brain with a high cellular turnover, such as the neurogenic centers at the subventricular zone (SVZ) or hippocampus, has yet to be elucidated. These regions contain subpopulations of neural stem cells (NSCs) able to differentiate into new neurons and glial cells throughout life.[12] O_2 is gaining increased recognition as a critical component of stem cell niches.[13,14] Quiescent somatic stem cells have a predominantly anaerobic metabolism, which helps to preserve them from excessive production of reactive oxygen species (ROS) and other stressors.[15] Recently, we have shown that peripheral NSCs in vitro are unaffected by hypoxia.[16,17] However, the actual effect of maintained hypoxic pO_2 values, such as those reached during extreme in vivo pathophysiological conditions, on brain NSC maintenance and differentiation is barely studied. Herein, we report the effect of chronic hypoxemia on the adult SVZ, a germinal layer lining the walls of the lateral ventricles in the brain,[18,19] and the adjacent striatum. NSCs in the SVZ generate large numbers of migrating neuroblasts and oligodendrocyte progenitors that could play a role in recovery after brain ischemia or myelin damage.[20–25] We show that NSCs as well as intermediate neuronal and oligodendrocyte progenitors at the SVZ are quite resistant to chronic hypoxia. Nonetheless, in this condition, the germinal layer undergoes a marked structural disarrangement that is accompanied by impairment of neuron and oligodendrocyte survival. Our data thus provide a new perspective on brain responsiveness to hypoxia, which is likely to be of significant medical relevance.

Materials and methods

Animals and hypoxic treatments

All experiments were performed according to institutional guidelines approved by the ethics committee of the Hospital Universitario Virgen del Rocío, the Animal Research Committee of the University of Seville, and the European Community (Council Directive 2010/63/EU). Wistar rats (2–3 months old) were used for the gasometry experiments. C57BL/6J mice (2–3 months old) were used in the other experiments presented in this study. Both were obtained from Charles River France and housed under temperature-controlled conditions (22°C) in a 12-hour light/dark cycle with free access to food and water. Animals were maintained in room air (normoxia, 21% O_2) or chronically exposed to hypoxia (10% or 8% O_2 environment) for 12–23 days by using a hermetic chamber enabling control of O_2 and CO_2 tensions as well as temperature and humidity (Coy Laboratory Products, Inc., Grass Lake, MI, USA). Control experiments were also performed with animals maintained within the chamber but at 21% O_2 (normoxic conditions). At the end of the experiment, each animal was deeply anesthetized with thiobarbital 0.6 g/kg body weight (B. Braun, Jaén, Spain). Systematic hematocrit analysis was performed with blood withdrawn from the vena cava. Then, the animals were either sacrificed by fixative perfusion for electron microscopy or immunohistochemistry or sacrificed by decapitation for tissue cell culture. For in vivo proliferation studies, the mice received a single intraperitoneal (ip) injection of 5-bromo-2'-deoxyuridine (BrdU) (50 mg/kg bw) after 12 days in the experimental conditions (Nx, 10% or 8%) and were sacrificed 1 hour later by perfusion. In the migration protocol, mice were ip injected with 50 mg/kg three times every 2 hours and were left in the normoxic or hypoxic conditions. These same mice were sacrificed by perfusion 11 days later, which is the delay for the cells generated in the SVZ to migrate to the olfactory bulb (OB) via the rostral migratory stream (RMS).

Gasometry and arterial blood parameters

Arterial blood was removed from the aorta of anesthetized normally breathing mice and rats using specific gasometry capillary tubes (catalog number 942-882; Radiometer Medical ApS, Brønshøj, Denmark) and immediately placed in a blood gas analyzer (ABL800 FLEX; Radiometer Medical ApS) to determine values for arterial pO_2, O_2 hemoglobin saturation, pH, pCO_2, and hemoglobin content. A hematocrit capillary (7311; DeltaLab, Barcelona, Spain) was also filled with arterial blood from the same animals. After 5 minutes of centrifugation in a small centrifuge (JP Selecta, Barcelona, Spain), hematocrit was determined by measuring cell volume as a percentage of the total blood volume.

Antibodies, special reagents, and immunostaining

For immunohistochemical and immunocytochemical studies, we followed procedures used before in our laboratory.[16,17,26] Details are given in the Supplementary materials.

Neurosphere assays

After 12 days in hypoxia or normoxia, the bilateral SVZ region (comprising surrounding striatal tissue) of freshly dissected brains was removed and kept in ice-cold sterile phosphate-buffered saline (PBS) until completing the dissections of the other animals in the experimental group. Each explant was cut into five to six smaller pieces and incubated for 30 minutes at 37°C and a 5% CO_2 atmosphere in Earle's balanced salt solution (24010, Gibco) containing

papain (30 U/mL, P4762, Sigma), supplemented with 1 mM L-cysteine and 0.5 mM ethylenediaminetetraacetic acid. Papain-incubated tissues were washed twice in Dulbecco's Modified Eagle's Medium-F12 (21331, Gibco) containing 100 U/mL penicillin–streptomycin, 1% N2, and 2% B27 supplements (Gibco), and cells were dissociated by passing through a tip-blushed glass pipette, centrifuged at 300× *g* for 5 minutes, and resuspended in neurosphere culture medium: Dulbecco's Modified Eagle's Medium-F12 with penicillin–streptomycin, N2, B27, 10 ng/mL basic fibroblast growth factor (bFGF, R&D Systems), 20 ng/mL epidermal growth factor (EGF, R&D Systems), and 0.7 U/mL heparin. After counting using a hemocytometer, cells were plated in ultralow-attachment six-well plates (Costar 3471, Corning) at a 2.5 cells/µL clonal density, that is, 500 cells/cm^2, to prevent neurosphere fusion.[27] Four technical replicates per animal were performed. Seven days after plating, the number of floating spheres per well was counted in each well, and the percentage of neurosphere-forming cells was calculated. For self-renewal assessment of primary neurospheres, SVZ-dispersed cells from normoxic mice (n=4) were plated at clonal density in the culture conditions described above and placed in incubators set at 5% CO_2 with 21%, 3%, 1%, or 0.5% O_2 concentrations. Six days after plating, the diameter of each sphere was measured under phase contrast with an inverted microscope (IX71 Olympus). Secondary neurospheres were obtained by incubating primary neurospheres prepared from SVZ cells removed from animals that had been maintained in normoxia or hypoxia (10% O_2) (n=6 each) with ready-to-use accutase solution (A6964, Sigma), for 20 minutes at room temperature (RT). Digestion activity was stopped by addition of three volumes of trypsin inhibitor solution (Supplementary materials). Cells were dissociated by passing through a tip-blushed glass pipette as described for the primary neurospheres. The subsequent steps were identical as for primary neurospheres formation (six technical replicates per animal). Six days after plating, the number of floating spheres was counted, and the percentage of neurosphere-forming cells was calculated.

For neurosphere differentiation assay and immunocytochemistry of stem cell-derived colony, glass coverslips in 24-well plates were treated, prior to plating, with 0.5 mg/mL human fibronectin (Biomedical Technologies) for adherence. Seven-day neurospheres from four normoxic SVZ were plated in the same culture medium as previously described but free from added mitogens (bFGF, EGF, heparin), and placed in 5% CO_2 incubators with 21%, 3%, or 1% O_2 levels. After 3 days or 7 days in differentiation conditions, cells were fixed for 20 minutes in 4% paraformaldehyde in the culture incubator, blocked in PBS with 0.1% Triton X-100 with 10% fetal bovine serum and 1 mg/mL bovine serum albumin, and then incubated overnight at 4°C with primary antibodies such as Tuj1, O4, and glial fibrillary acidic protein (GFAP) to label neurons, oligodendrocytes, and astrocytes, respectively. After extensive rinses, cells were placed with Alexa® fluorophore-conjugated anti-IgG for 1 hour at RT. Finally, cells were counterstained with 0.5 µg/mL 4′,6-diamidino-2-phenylindole dihydrochloride (Dapi) for 10 minutes at RT, and coverslips mounted on slides with Fluoro-gel. Four to six photos per animal for each staining, plus Dapi, were acquired with the ×20 objective. Images were processed, and Tuj1-, O4-, and GFAP-positive cells were counted with Photoshop CS5, and divided by the total number of Dapi-positive cells in the respective field to obtain a percentage of Tuj1+, O4+, and GFAP+ cells.

Electron microscopy

Mice were intracardially perfused with PBS followed by 2% paraformaldehyde and 2.5% glutaraldehyde (EMS, Hatfield, PA, USA) in PBS pH 7.4, and the brains were incubated for 16 hours in the same fixative at 4°C. Following fixation, brains were washed in 0.1 M phosphate buffer (PB) pH 7.4, cut into 200 µm thick sections with a vibratome (VT 1000 M, Leica, Wetzlar, Germany), and treated with 2% osmium tetroxide in PB for 2 hours. Sections were then rinsed, dehydrated through increasing ethanol solutions, and stained with 2% uranyl acetate at 70% ethanol. Following dehydration, slices were embedded in araldite (Durcupan, Fluka Bio-Chemika, Ronkonkoma, NY, USA). To study the cellular organization of the SVZ germinal niche, serial 1.5 µm thick semithin sections were cut with a diamond knife and stained with 1% toluidine blue. To identify and quantify cell types and structural alterations in the SVZ, as well as to analyze myelin sheaths in the striatum, 60–70 nm thick ultrathin sections were cut with a diamond knife, stained with lead citrate, and examined under a Spirit transmission electron microscope (FEI Tecnai, Hillsboro, OR, USA). SVZ cell-type identification was performed as previously described.[28] For quantitative analysis, three different anteroposterior levels were analyzed per animal and n=3 per group (Nx, 8% and ReNx). Data are reported as the mean ± standard error of the mean (SEM). The applanation index was estimated by dividing the ependymal layer area (measured with ImageJ; Rasband WS. ImageJ. Bethesda, MD: US National Institutes of Health; 1997–2014. Available from: http://imagej.nih.gov/ij/) by the number of nuclei. Three different anteroposterior levels were selected per animal and n=3 per group (Nx, 8% and ReNx). Data are reported as the mean ± SEM.

Myelin destructuration index

To measure alteration in the myelin sheets, the destructuration index was estimated by dividing the number of axons with affected myelin sheets by the total axon number and then divided by the frame area (20.8 μm^2). Three different anteroposterior levels of the dorsomedial striatum (DMS) were selected per animal, and at each level, ten pictures of the axon bundles were randomly obtained at the same magnification (×20,500) for quantification (Nx, n=6; 10% O_2, n=3; 8% O_2, n=3; ReNx, n=3). Data are reported as the mean ± SEM.

Statistical analysis

Statistical comparisons were performed by using PASW Statistics 17.0 software. Before statistical analysis, percentages were subjected to arc-sine transformation to convert them from a binomial to a normal distribution. Comparison between two groups was subjected to an unpaired Student's *t*-test. One-way analysis of variance followed by the Bonferroni post hoc multiple comparisons test was used to draw comparisons between three or more groups. The level of significance was set at $P<0.05$.

Results

Hypoxia induces nonreversible structural alterations in SVZ

Animals acclimatized and survived well in the hypoxic conditions, thanks to hyperventilation and an increased hematocrit that was inversely proportional to the level of O_2 tension (Table 1). Animals maintained in hypoxia were relatively hypokinetic but did not show signs of distress. Although most of the data presented here were obtained from mice, the modifications in blood gases and pH during exposure to hypoxia were estimated in rats, which showed qualitatively similar SVZ responses and have higher total blood volume than mice. Environmental hypoxia (10% O_2 for 12 days) led to a severe normocapnic hypoxemia (~50 mmHg arterial pO_2) and a marked decrease in the level of hemoglobin saturation (<70%). Blood pH slightly decreased in animals exposed to hypoxia, but the change was not statistically significant (Table 1).

Hypoxia induced a marked angiogenesis and pronounced remodeling of the brain parenchyma in the dorsomedial striatum adjacent to the SVZ, which recovered only partially upon returning to normoxia (renormoxia) (Figure 1A and B). Angiogenesis was manifested by increase in the area occupied by blood vessels, as well as by the average size and number of capillaries (Figure 1C). Interestingly, high-magnification electron microscope (EM) analysis revealed profound ultrastructural alterations at the SVZ induced by hypoxemia. The most notable and consistent changes were flattening of the ependymal cell layer and the presence of enlarged blood vessels in the SVZ, which sometimes were anomalously observed in close contact with ependymal cells, a very rare situation in normoxic animals (Figure 1D–F). In addition, displaced striatal neurons and axon bundles adjacent to the ependymal cell layer (Figure 1D, E, and G) were seen throughout all levels in the ventricular area. Other abnormal features observed at various levels of hypoxia were thinning of capillary walls (Figure 1H) and the presence of numerous pyknotic cells (Figure 1I). Ectopic striatal neurons persisted 12 days after returning to normoxia (Figure 1D and E), which may indicate long-lasting modifications of the SVZ in individuals exposed to sustained hypoxia.

Table 1 Blood parameters in chronic hypoxia animals

	Normoxia	Hypoxia 10% (12 days)	Hypoxia 9% (12 days)	Hypoxia 8% (12 days)	Hypoxia 8% (23 days)
Hematocrit and body weight in the hypoxic mouse models					
Hematocrit (%)	48.72±0.94	68.56±1.42***	79.79±0.73***	82.90±0.90***	93.36±0.64***
Body weight difference with normoxia	–	−14.33%***	−13.21%***	−13.25%***	−19.60%***
N	5	5	5	5	5
Arterial blood gasometry in rats	**Normoxia (air)**		**Normoxia (chamber 12 days)**	**Hypoxia 10% (12 days)**	
Hematocrit (%)	48.5±1.1		48.1±1.5	61.3±2.3***	
O_2 saturation (%)	95.5±0.4		95.7±0.6	67.6±7.3	
pO_2 (mmHg)	108.2±2.9		104.6±3.5	50.0±1.9***	
pCO_2 (mmHg)	44.0±1.5		40.7±0.3	44.9±2.7	
Hemoglobin (g/dL)	16.0±0.3		15.2±0.0	17.6±0.4*	
pH	7.35±0.02		7.38±0.00	7.28±0.03	
N	8		3	2	

Note: *$P<0.05$ versus normoxia and ***$P<0.001$ versus normoxia; one-way analysis of variance and Bonferroni post hoc test.

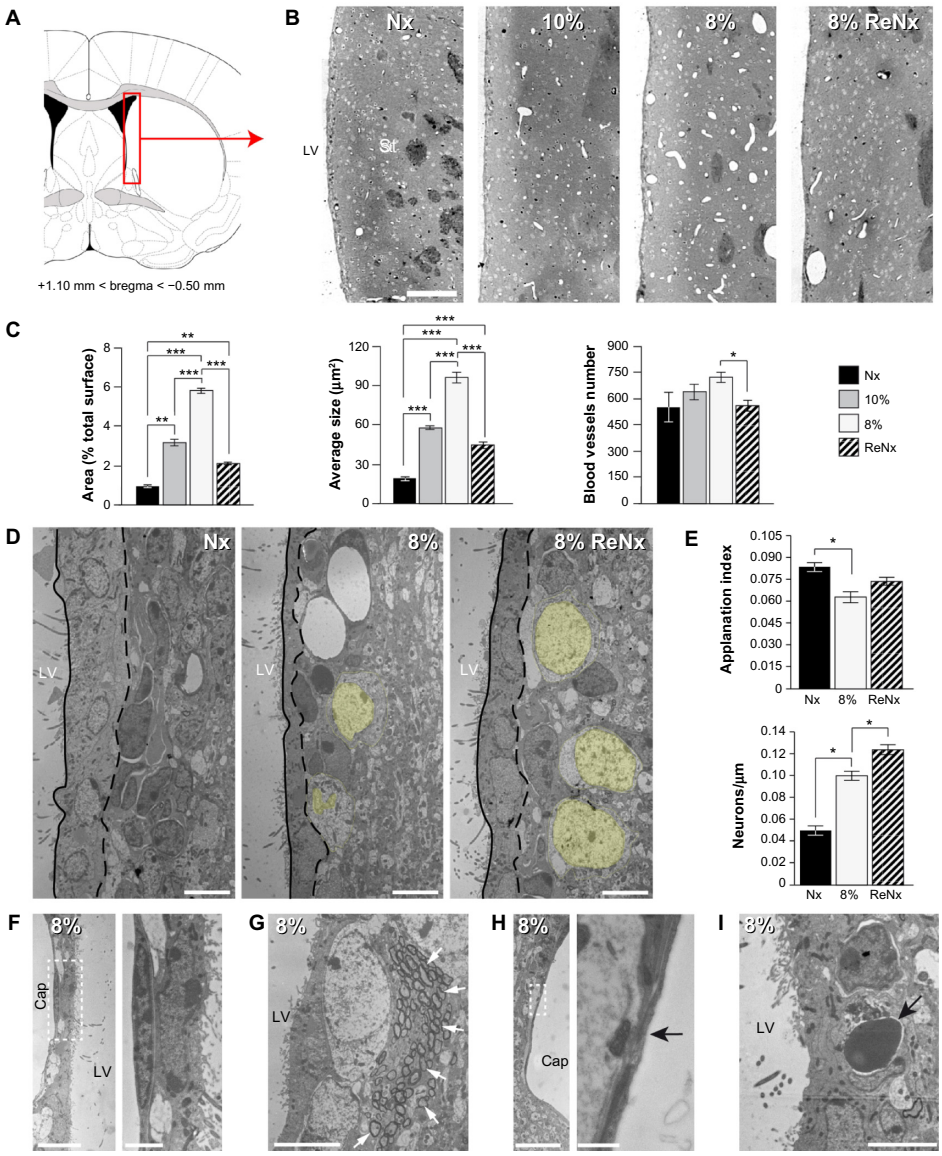

Figure 1 Ultrastructural appearance of the subventricular germinal zone in chronic hypoxia.

Notes: (**A**) Localization of the SVZ in the mouse brain (from the Paxinos and Franklin's Mouse Brain Atlas). The rostro-caudal limits of the SVZ considered for quantification, with respect to bregma, are indicated. Scale bar =100 µm. (**B**) Semithin sections of the striatal region (St) adjacent to the lateral ventricle (LV) illustrating the increased presence of blood vessels in animals maintained at 10% (12 days) and 8% (12 days) hypoxia. Large blood vessels were still observed after animals were maintained in a normoxic (Nx) atmosphere (21% O_2) for 12 days (8% ReNx). (**C**) Angiogenesis quantification presents an increase in the surface (left bargraph; n=3) and the average size (middle bargraph; n=3) of the blood vessels at 10% and 8% O_2 tension. After 12 days of renormoxia (ReNx), animals only partially recovered the angiogenesis observed in 8% hypoxia. Number of blood vessels (right bargraph) increased (nonsignificantly) in hypoxia and significantly decreased after renormoxia (n=3). (**D**) Representative electron microphotographs of the SVZ showing diminution of the ependymal layer width in 8% hypoxia (between dotted and plain lines). Displaced neurons at 8% hypoxia and post-8% renormoxia are highlighted in yellow. Scale bar =6 µm. (**E**) Quantitative analysis of ependymal layer flattening (applanation index; in arbitrary units, upper bargraph) (n=3) and the number of displaced neurons per micrometer in the SVZ layer (lower bargraph) (n=3). (**F–I**) Electron microphotographs illustrating 8% hypoxia-induced SVZ alterations. (**F**) Direct contact between a blood capillary (Cap) evidenced by the elongated shape nucleus of the endothelial cell (on the left-hand side) and ependymocyte (cuboidal nucleus with microvilli). Scale bar =8 µm, inset =2 µm. (**G**) Displaced striatal bundle of myelinated axons (white arrows) near the ventricle. Scale bar =6 µm. (**H**) Thinning of the endothelial membrane (horizontal black arrow). Scale bar =8 µm, inset =80 nm. (**I**) Pyknotic cells are also observed in the SVZ (black arrow). Scale bar =4 µm. *$P<0.05$, **$P<0.01$, and ***$P<0.001$.

Abbreviations: Cap, capillary; LV, lateral ventricle; SVZ, subventricular zone.

NSCs and intermediate progenitors at the SVZ niche are resistant to hypoxia

The ultrastructural abnormalities observed in the SVZ lead us to further investigate a possible effect of hypoxia on the proliferative germinal center. The SVZ contains four main cell types defined by their morphology, ultrastructure, and molecular markers: migrating neuroblasts (type A cells), astrocytes (type B cells), proliferative precursors (type C cells), and ependymal cells (type E cells). It has been shown that a subpopulation of B-cells are the primary NSCs, which

are converted to transient amplifying type C cells that generate neuroblasts and glial cells.[18,19] Neuroblasts arranged in chains migrate tangentially along the RMS to the OB, where they differentiate into mature interneurons. The cell classes characteristic of SVZ are illustrated by semithin sections in Figure 2A (left) that also show blood vessels within the SVZ at 8% O_2 tension and the presence of abnormal intercellular gaps in renormoxia. However, the number of the various cell types in the SVZ identified in ultrathin EM sections was not significantly affected even by severe (8% O_2) hypoxia (Figure 2A, right). The SVZ dissected from normoxic and chronically hypoxic animals showed a similar ability to generate primary and secondary neurospheres (Figure 2B), thus further supporting the view that SVZ progenitors (B- and C-type cells) are unaffected by hypoxia. Indeed, SVZ-derived neurosphere diameter, an indication of proliferative activity of progenitor cells,[16] was unaffected by a broad range of O_2 tensions (1%, 3%, and 21%). Progenitor proliferation only decreased significantly when the neurospheres were exposed to extreme low pO_2 values (0.5% or ~3 mmHg) (Figure 2C).

In parallel to the neurosphere experiments, we examined the in vivo proliferation activity of cells in the anterior horn of SVZ by means of the administration of BrdU to animals as well as the immunocytochemical detection of the proliferating cell nuclear antigen (PCNA), a broader marker of proliferating cells. Unbiased counting of stained cells with the two methods revealed no difference between normoxic and hypoxic mice (Figure 2D and E). The number of BrdU+ cells remaining in SVZ 11 days after injection of the marker (an indication of B-type cell number[29]) as well as the intensity of GFAP+ staining at SVZ was unchanged by hypoxia (Figure S1), thus supporting the data obtained by direct counting of B-type cells in ultrathin EM sections. The number of neuroblasts (A-type cells), as determined by the specific marker doublecortin,[30] was also similar in hypoxic and normoxic animals (Figure 2F). Taken together, these data suggest that in spite of the profound structural alterations induced by hypoxia in the SVZ, the cellular components of the germinal niche (stem cells, transient amplifying progenitors, and neuroblasts) are insensitive to chronic severe (up to 8% O_2 for 12 days) hypoxic treatment.

Chronic hypoxia reduces survival of newborn neurons in vivo and in vitro

Newborn neuroblasts in the anterior SVZ migrate toward the OB, where they differentiate into young neurons in either the granule cell layer (GCL) or periglomerular layer.[31,32] EM observations of the RMS indicated that neuroblast migration was not altered after 12 days at 8% O_2 (Figure 3A). This was also confirmed by experiments in which after 12 days in hypoxia, animals were injected with BrdU and sacrificed 11 days later. With this protocol, BrdU+ neuroblasts born at the SVZ were located at the GCL in maturation stage 3 at the moment of sacrifice.[32,33] Hypoxic treatments (8% or 10% O_2) produced a decreasing trend in the number of BrdU+ cells (most of them maturating neuroblasts) at OB; however, the differences were not statistically significant (Figure 3B). We further investigated the nature of BrdU+ cells at the OB and found that the number of double BrdU+ and NeuN+ (neuronal nuclei, a neuronal marker) cells clearly decreased in mice treated with either 10% or 8% O_2 tensions, whereas the number of BrdU+ and NeuN− cells remained unaltered (Figure 3C). In normoxia, at least half of the BrdU+ cells at GCL were in the process of neuronal maturation (NeuN+), but during exposure to hypoxia, this occurred only to a third of the cells (Figure 3D). In animals that stayed for 23 days in hypoxia, cell counts in the GCL indicated that exposure to 8% O_2 tension produced a selective decrease in the number of neurons (NeuN+ cells) at the GCL in parallel with an increase in the number of moon-shaped nuclei, presumably endothelial cells, which confirms the hypoxic condition of these mice (Figure 4A). Hypoxia also induced an increase in cell apoptosis at the OB that was not seen in other parts of the brain, as, for example, the striatum (Figure 4B). These results suggest that SVZ newborn neuroblasts can migrate normally through the RMS in severe chronic hypoxia, but once arrived in the OB, their differentiation into neurons or survival of newly differentiated neuronal cells is compromised.

The effect of lowering pO_2 on differentiation of SVZ progenitors was further investigated in vitro by culturing neurospheres in differentiation media and plating on adherent substrate. Moderate hypoxia (3% O_2) had no effect on the number of Tuj1+ cells generated from neural progenitors. However, more severe hypoxia (1% O_2), probably similar to the O_2 levels likely reached in the OB of animals maintained in hypoxia, resulted in a dramatic decrease in the survival of neurons once they were generated. Under the same in vitro conditions, GFAP+ astrocytes were unaffected (Figure 5A).

Oligodendrocyte damage in chronic hypoxia

Besides neuroblasts and astrocytes, multipotent progenitor cells in SVZ neurospheres were also able to generate oligodendrocytes, the survival of which was also compromised in extreme hypoxic conditions (Figure 5B). The inhibition

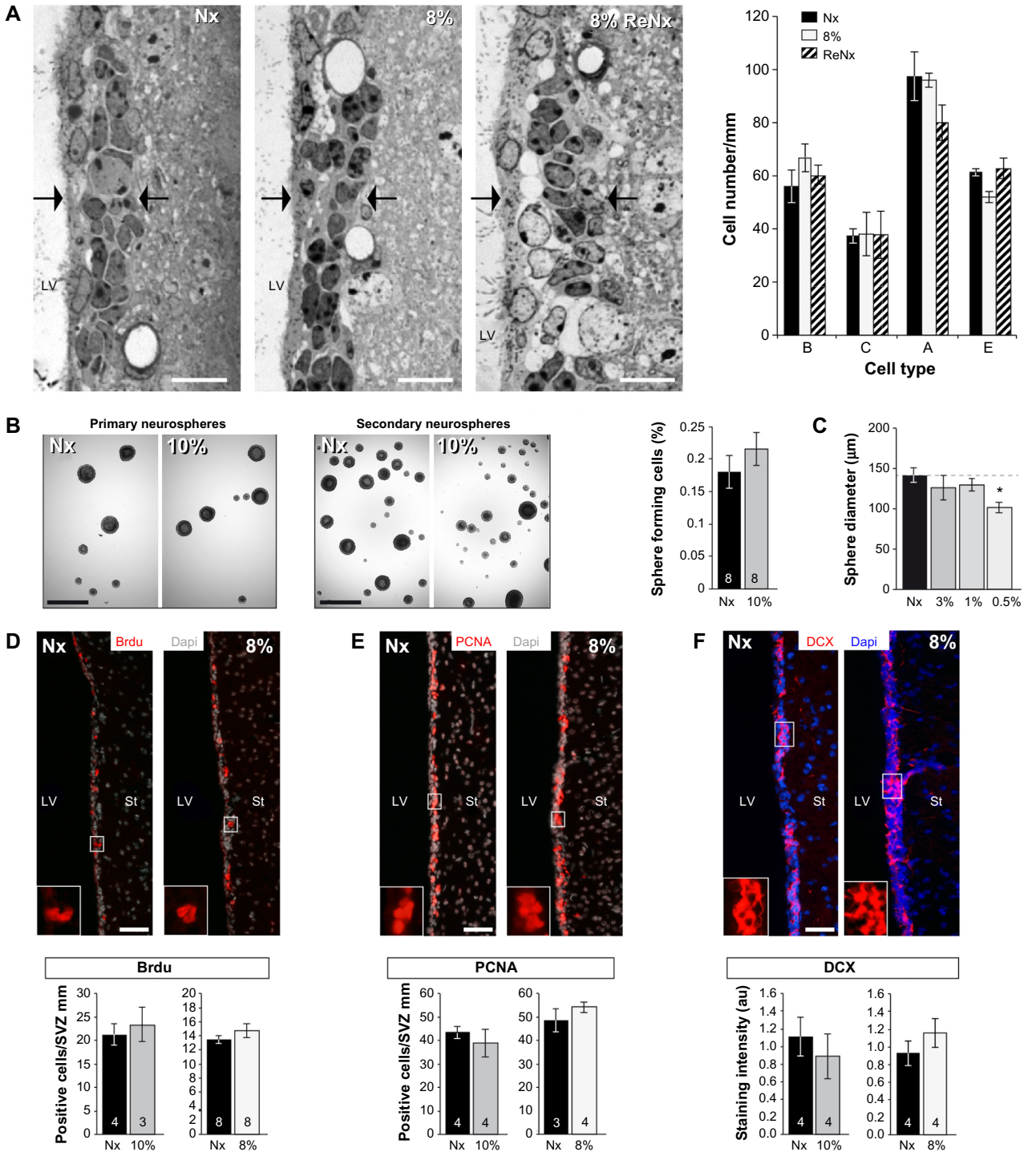

Figure 2 Cell proliferation in the SVZ is resistant to chronic hypoxia.

Notes: (**A**) Semithin section photographs of the SVZ in normoxia (Nx), 8% hypoxia (12 days), and renormoxia following 12 days in 8% hypoxia (ReNx). The SVZ width is indicated between the two black arrows. Scale bar =10 µm. The bargraph (right) indicates the mean ± SEM number of the different cell types that form the germinal niche (n=3 per condition). (**B**) Primary and secondary neurospheres culture from the SVZ region. Low-magnification photographs show the neurospheres formed in a 35 mm dish at clonal density. Scale bar =1 mm. The vertical bargraphs (right) indicate the percentage of sphere-forming cells from mouse SVZ sacrificed in Nx or after 12 days at 10% hypoxia (primary neurospheres), and the percentage of sphere-forming cells after dispersion of the primary neurospheres. The number of individuals is shown at the bottom of each vertical bar. (**C**) Mean diameter (± SEM) of primary neurospheres cultured at different oxygen levels. The spheres diameter decreased significantly only at a very low O_2 concentration of 0.5%. *$P<0.05$, n=4. (**D**–**F**) Proliferation markers show no evidence of hypoxia effect on proliferation in vivo. Representative microphotographs illustrating (**D**) BrdU, (**E**) PCNA, and (**F**) DCX staining in normoxia (Nx) and 8% hypoxia. Quantification results are presented below. (**D**) Mean ± SEM BrdU-positive cells at 10% and 8% hypoxia. Scale bar =20 µm. (**E**) Mean ± SEM PCNA-positive cells at 10% and 8% hypoxia versus normoxia. Scale bar =20 µm. (**F**) DCX staining intensity at 10% and 8% hypoxia. Scale bar =15 µm. The number of individuals per condition is shown at the bottom of each vertical bar.

Abbreviations: SVZ, subventricular zone; SEM, standard error of the mean; BrdU, 5-bromo-2'-deoxyuridine; PCNA, proliferating cell nuclear antigen; DCX, doublecortin; au, arbitrary unit; LV, lateral ventricle; Dapi, 4′,6-diamidino-2-phenylindole dihydrochloride; St, striatal region.

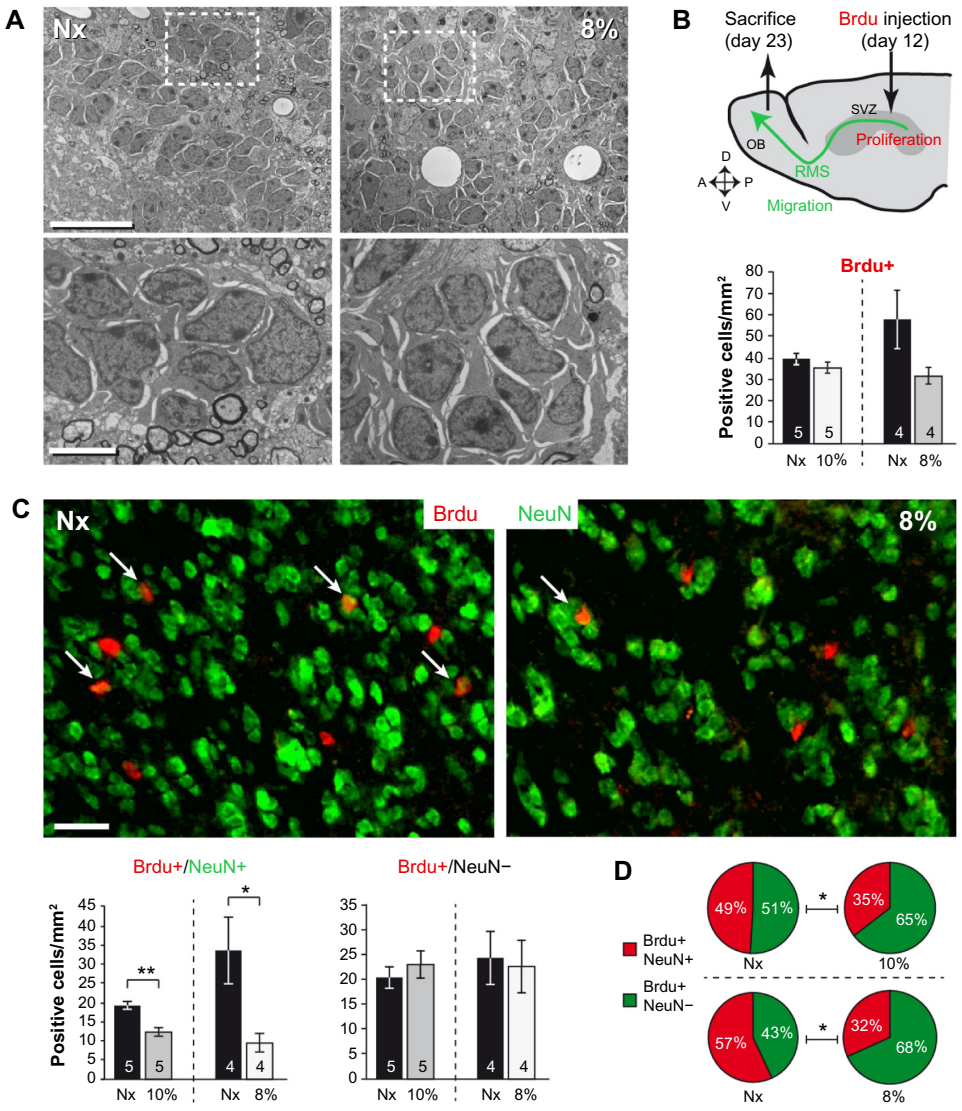

Figure 3 Chronic hypoxia affects neuroblast differentiation in the OB.

Notes: (**A**) Electron microphotographs of neuroblasts chain in the RMS displaying similar morphology but dilated intracellular spaces in 8% hypoxia. Squared areas (white dotted lined) are shown at greater magnification. Scale bar =10 µm, inset =2 µm. (**B**) Illustration of the BrdU injection strategy. BrdU (3×50 mg/kg) was injected after 12 days in hypoxia or normoxia. BrdU-positive cells generated in the SVZ migrated for 11 days through the RMS to reach the OB. Vertical bars indicate the number of BrdU-positive cells in the GCL of the OB at 10% hypoxia versus normoxia (Nx) or 8% hypoxia versus normoxia. The number of individuals per condition is shown at the bottom of each vertical bar. (**C**) Photomicrographs show BrdU+ (red) and NeuN+ (green) cells in the GCL in normoxia or 8% hypoxia. White arrows point at double-stained BrdU+/NeuN+ cells. Scale bar =20 µm. Vertical bargraphs indicate the number of BrdU+ cells (± SEM) that have differentiated into NeuN+ neurons (left bargraph), or that remain NeuN– (right bargraph). (**D**) Circular diagrams illustrating the difference of BrdU+ cells differentiated into NeuN+ cells (red) or that remain NeuN– (green) between normoxia and 10% or 8% hypoxia, respectively, expressed as percentage of total BrdU+ cells. *$P<0.05$ and **$P<0.01$.

Abbreviations: OB, olfactory bulb; RMS, rostral migratory stream; BrdU, 5-bromo-2'-deoxyuridine; SVZ, subventricular zone; GCL, granule cell layer; NeuN, neuronal nuclei; SEM, standard error of the mean.

of neuronal or oligodendrocyte survival in severe hypoxia (1% O_2) in vitro was also observed in secondary neurospheres regardless of whether the original progenitors came from animals that had been maintained in normoxic (21% O_2) or hypoxic (10% O_2) conditions (Figure S2).

We tested whether chronic hypoxia also damaged oligodendrocytes in vivo. Adult SVZ progenitors are known to migrate to neighboring white matter bundles to generate oligodendrocyte precursors.[22,23,25] Hence, we analyzed oligodendrocyte precursors, oligodendrocytes, and myelin bundles in a region of the DMS adjacent to the SVZ within 300 µm from the border of the lateral ventricle. Chronic exposure to low pO_2 (down to 8%) did not produce any difference in the number of oligodendrocyte precursors (NG2-expressing cells) in the DMS (Figure 6A). The number of NG2+ cells in dorsolateral striatum and motor cortex also remained unaffected by hypoxia (Figure S3). However, lowering pO_2 resulted in a decrease in striatal oligodendrocyte (Olig+) number, which was proportional to the severity of hypoxia. The number of Olig+ cells decreased to half after 23 days of

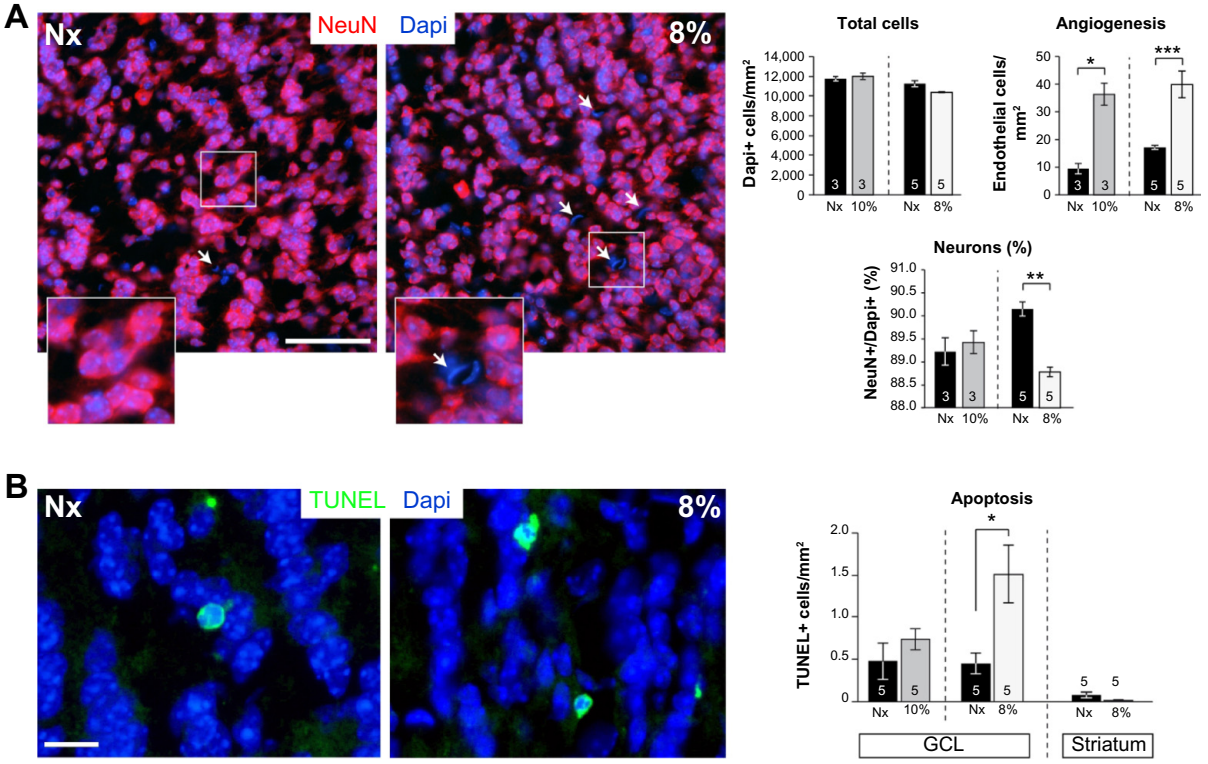

Figure 4 Neuronal loss from apoptosis in the olfactory bulb in severe chronic hypoxia.

Notes: (**A**) Coronal sections of the olfactory bulb GCL indicating NeuN+ cells (red) and total cell number (Dapi, blue). Besides a general, but not significant, loss of cells (Dapi+), the number of neurons (NeuN+ cells) decreased after 23 days in 8% but not in 10% O_2. Note that angiogenesis (indicated by the increased number of endothelial cells with moon-shaped nuclei) is observed at both 10% and 8% hypoxia (white arrows). Scale bar =50 μm. The insets show the indicated areas at higher magnification. The number of individuals per condition is shown at the bottom of each vertical bar. (**B**) Histological sections of the olfactory bulb GCL indicating TUNEL+ cells (green) and total cell number (Dapi, blue) in normoxic animals (left) and in animals exposed to 8% O_2 for 12 days (right). The vertical bargraph shows the mean number ± SEM of TUNEL+ cells per squared mm. The number of individuals per condition is shown at the bottom of each vertical bar. Significant increase in apoptotic cells is observed at 8% hypoxia versus normoxia (Nx). TUNEL+ cells are rarely found in the striatum of both normoxic and hypoxic (8% O_2) animals. *P<0.05, **P<0.01, and ***P<0.001.

Abbreviations: GCL, granule cell layer; NeuN, neuronal nuclei; Dapi, 4′,6-diamidino-2-phenylindole dihydrochloride; SEM, standard error of the mean.

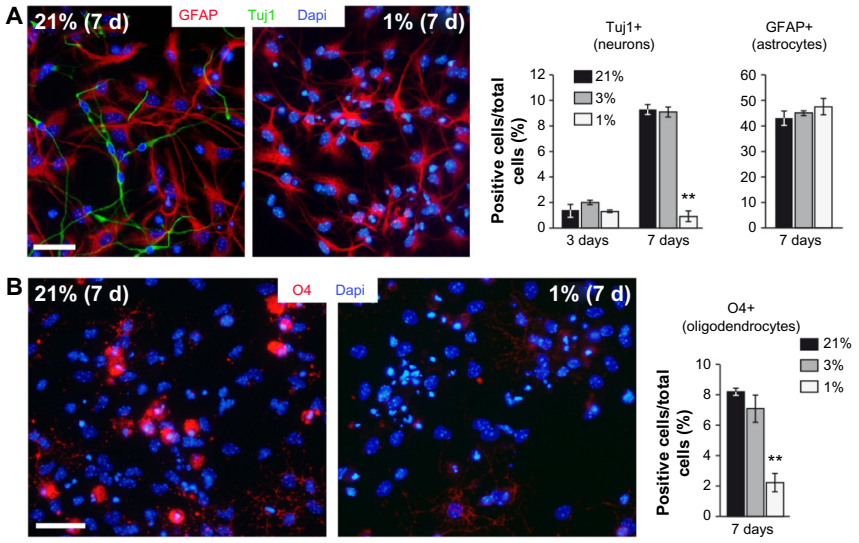

Figure 5 In vitro SVZ progenitors differentiation and survival.

Notes: (**A**) Microphotographs of SVZ neurospheres, cultured at variable levels of O_2 tension, after 7 days in differentiation medium: neurons (Tuj1+, green), astrocytes (GFAP+, red), and nuclei (Dapi, blue). Scale bar =30 μm. Bargraphs indicate the selective decrease of neurons after 7 days in culture at 1% O_2. The number of GFAP+ cells (astrocytes) remains unchanged in the three different O_2 tensions tested (n=4 per condition). (**B**) Microphotographs of SVZ neurospheres, cultured at variable levels of O_2 tension, after 7 days in differentiation medium: oligodendrocytes (O4, red) and nuclei (Dapi, blue). Scale bar =30 μm. Vertical bargraph shows the percentage of O4+ cells after 7 days in culture at three different levels of O_2 tension. **P<0.01.

Abbreviations: SVZ, subventricular zone; GFAP, glial fibrillary acidic protein; Dapi, 4′,6-diamidino-2-phenylindole dihydrochloride.

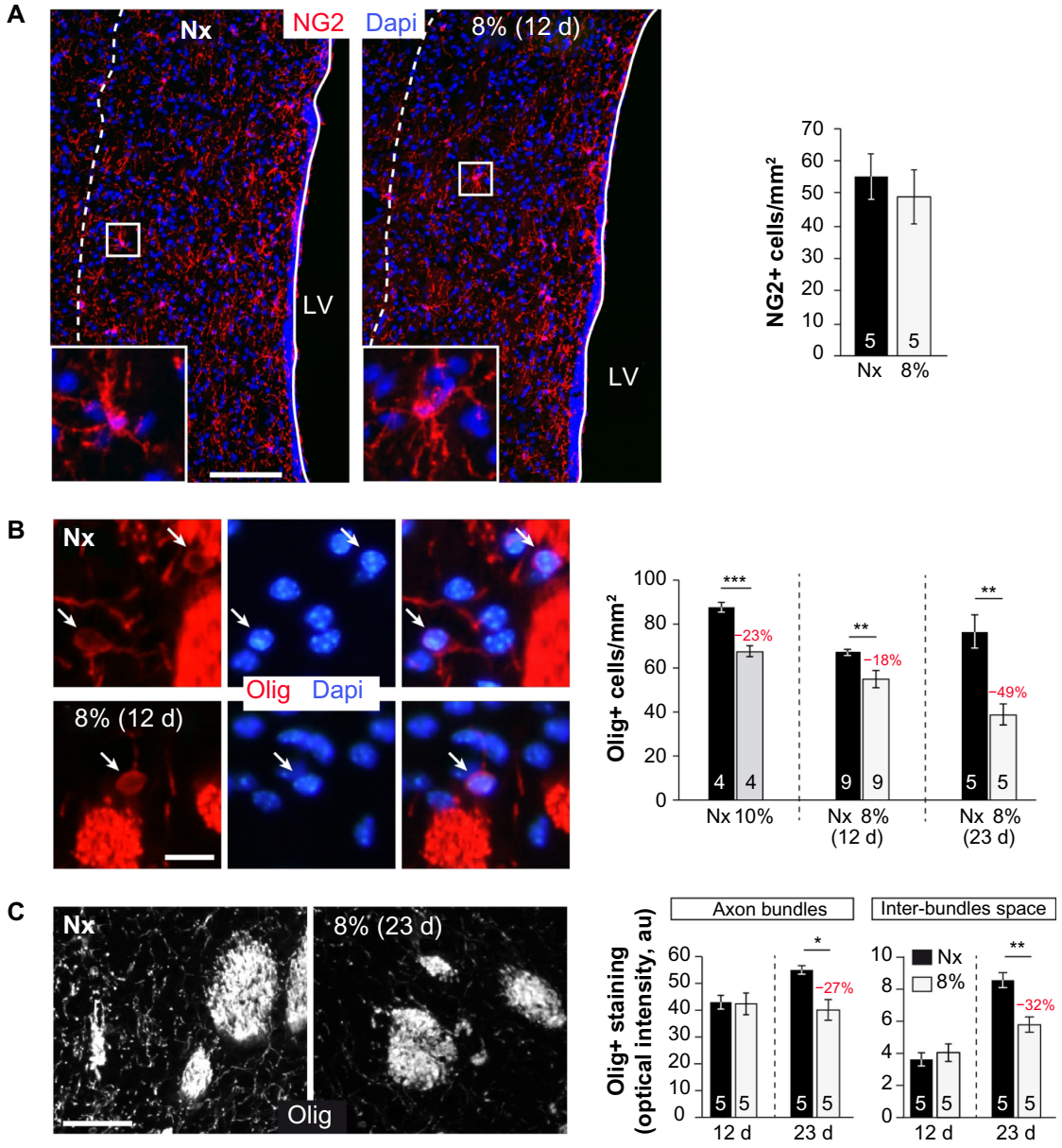

Figure 6 Oligodendrocytes cell loss and demyelination in chronic hypoxia.

Notes: (**A**) Coronal sections of SVZ and neighboring striatum showing oligodendrocyte progenitors (NG2+ cells, red) in normoxic and hypoxic animals. The discontinuous line marks a striatal region of 300 μm from the ependymal layer. Scale bar =100 μm. Inset shows the indicated regions at higher magnification. The bargraph shows that the number of immature oligodendrocytes progenitors is not affected by 12 days in 8% hypoxia. (**B**) The high-magnification photographs in the medio-dorsal striatum illustrate the loss of mature oligodendrocytes (Olig+ cells, red) at 8% O_2 (12 days) versus normoxia. Only oligodendrocytes with Dapi-positive nuclei (blue) located outside of the axon bundles were quantified (arrows). Scale bar =10 μm. Vertical bargraphs show the number of cells per square millimeter in animals maintained at 10% and 8% O_2 tension (12 days or 23 days duration) versus their normoxic littermates. Red values indicate the percent decrease from the normoxic counterparts. The number of individuals per condition is shown at the bottom of each vertical bar. (**C**) Olig staining optical density decreases with increased chronic hypoxia. Representative photomicrographs (after grayscale image processing) show decreased Olig staining in the striatum after 23 days at 8% O_2 tension. Scale bar =40 μm. Vertical bargraphs indicate the Olig staining optical density inside (left) and between (right) the striatal axon bundles. Values in red indicate the percentage of decrease from the normoxic counterparts. *P<0.05, **P<0.01, and ***P<0.001.

Abbreviations: SVZ, subventricular zone; Dapi, 4′,6-diamidino-2-phenylindole dihydrochloride; LV, lateral ventricle.

exposure to 8% O_2 tension (Figure 6B). Interestingly, whereas the number of axon bundles remained unchanged, the surface area occupied by them as well as the intensity of myelin staining within the striatal axon bundles markedly diminished with the degree and duration of hypoxia (Figures 6C, S4, and S5). These findings, suggesting oligodendrocyte damage and loss of myelin, were further supported by ultrastructural studies showing striking disruptions of the myelin sheaths that progressed with the level of hypoxia and remained after recovery in normoxia (Figure 7). These alterations were accompanied by axon degeneration and cellular debris. The destructuration index, a parameter that estimated the degree of affectation of myelinated axons, indicated a hypoxia-induced damage of the myelin structure (Figure 7). In summary, our in vitro

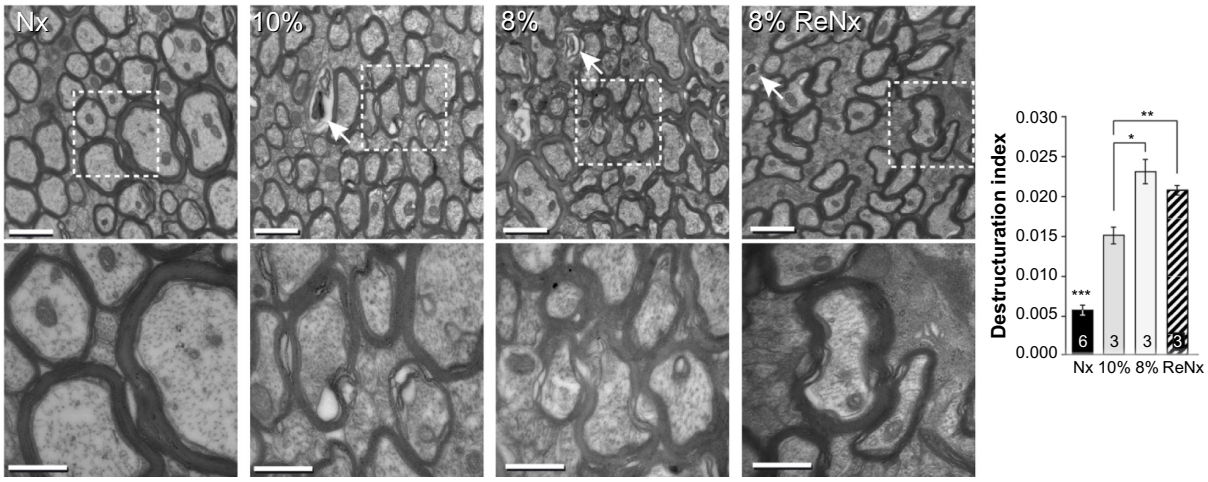

Figure 7 Myelin destructuration in the mouse striatum exposed to chronic hypoxia.
Notes: Top: electron photomicrographs showing myelinated axons within striatal bundles. The areas indicated are shown at the bottom at higher magnification. In normoxia (Nx), the myelin is continuously compact around axons. However, after 12 days in 10% or 8% hypoxia or post-8% renormoxia (ReNx), myelin sheaths appear loose around many axons. Note the presence of vacuoles containing cellular debris (white arrows). Scale bar =1 μm, inset =500 nm. The vertical bargraph represents the destructuration index calculated for each condition. *$P<0.05$, **$P<0.01$, and ***$P<0.001$ versus all other conditions.

and in vivo results highlighted a dramatic effect of low O_2 tension on mature oligodendrocyte homeostasis in the adult mouse striatum.

Discussion

There are numerous studies describing the effect of focal ischemia or acute hypoxia on brain cells[20,34,35] as well as the brain developmental deficits induced by perinatal deficit of O_2.[36–39] However, the effect of chronic hypoxia on adult germinal centers has not as yet been investigated in detail. We have shown that rodents exposed to low environmental O_2 for several days or weeks develop a syndrome that is characterized by chronic hypoxemia, erythrocytosis, and blood hemoglobin desaturation similar to that present in medical conditions such as COPD[3,4] or chronic mountain sickness.[2,10] Using this model, we have found that chronic hypoxemia induces a marked angiogenesis and profound structural disarrangement of the SVZ. Unexpectedly, this condition did not seem to damage NSCs and intermediate progenitors at the subventricular germinal center. However, chronic hypoxia decreased the survival of newly generated neurons and oligodendrocytes, with damage of myelin sheaths.

Chronic hypoxia elicited a marked ultrastructural disarrangement in the SVZ, which was typically characterized by thinning of the ependymal layer, and displacement of striatal neurons and myelinated axons toward the ependyma. These alterations, accompanied by strong angiogenesis and an attenuation of the capillaries, are probably the result of increased tension of the striatal parenchyma upon the ventricle wall secondary to the increase in the area occupied by blood vessels. Notably, hypoxia-induced alterations in SVZ ultrastructure were only partially reversible, and some remained even 3 weeks after resuming to normoxia. Despite these histological changes, the number of identified NSCs (B-cells), intermediate progenitors (C-cells), and neuroblasts (A-cells) in the SVZ, as well as oligodendrocyte progenitors (NG2+ cells) in the neighboring striatum, was unchanged in animals exposed to hypoxia (down up to 8% O_2 tension). Moreover, the number of proliferating cells in the germinal layer was also unaltered in animals exposed to low pO_2. In accord with these in vivo observations, we also observed a similar number of neurosphere-forming cells derived from the SVZ of hypoxic animals compared to controls. In addition, the growth of SVZ-derived neurospheres in vitro was unaffected by variations of O_2 tension in the range between 1% and 21%. Taken together, these findings suggest that NSCs, immature progenitors, and neuroblasts are resistant to hypoxia. This is in accord with a considerable body of recent knowledge indicating that both embryonic and adult stem cells or progenitor cells rely predominantly on a non-aerobic metabolism, which preserves them from oxidative stress.[14,15,40] Similar to NSCs in the SVZ, we have also shown that neural crest-derived progenitor cells in the carotid body are also insensitive to hypoxia.[16] Numerous studies in rodents and primates have reported an increase in the proliferation of neural progenitors in the SVZ or hippocampus in response to brain injury (most commonly experimental stroke after focal cerebral ischemia), and the migration of neuroblasts to the damaged brain parenchyma.[20,41–43] An increase in cell proliferation and neuroblast number has also been observed in the human SVZ after ischemic stroke.[24]

However, this response to ischemia, which is probably due to the release of chemotactic pro-inflammatory agents in the injured area, is transient and has only minor restorative capacity as most of the newly generated cells are short-lived and nonfunctional.[44] In agreement with these observations, it has recently been reported that short exposure to environmental hypoxia (10% O_2 for 6–72 hours) induces proliferation (without increasing differentiation) of hippocampal NSCs,[45] and we have observed a similar phenomenon in SVZ (data not shown). However, these short-lasting (hours) exposures to hypoxia are different from the chronic treatments lasting weeks, in which angiogenesis and structural rearrangements of brain structures are fully developed.

Although chronic hypoxia did not seem to affect the maintenance and proliferation of neural progenitors in SVZ, our in vivo and in vitro experiments indicate that survival of neurons and oligodendrocytes was compromised, whereas GFAP+ astrocytes were preserved. Exposure to hypoxia, particularly to 8% O_2, decreased the number of BrdU+ and NeuN+ cells and selectively increased apoptosis in the OB in comparison with the striatum, thus suggesting the loss of newly generated neurons. Under normal conditions (21% O_2), O_2 tension in most brain areas is estimated to be 2%–6%,[5] a range of values considered as "mild hypoxia". These O_2 levels are known to favor differentiation of neuronal progenitors in vitro.[46,47] However, O_2 tension in some brain regions surely decreases to near 1% or below in rodents chronically exposed to severe low environmental pO_2, and whose arterial O_2 tension drops from 100 mmHg to nearly 50 mmHg. Indeed, our data indicate that survival of differentiated neurons and oligodendrocytes is unaffected in SVZ-derived neurospheres cultured in 3% O_2 but drastically reduced in 1% O_2. The O_2 level necessary to prevent cell damage seems to be particularly high for oligodendrocytes, since their number was significantly decreased in animals exposed to relatively mild hypoxia (10% O_2 for 12 days). Hypoxia also markedly reduced myelin expression and altered the ultrastructure of myelin sheaths. These observations fit with previous studies describing the high-energy demands of oligodendrocytes and their particular sensitivity to ischemic damage (for review and references, see Bradl and Lassmann[48]). Oligodendrocytes are also highly vulnerable to oxidative stress due to their elevated iron content and relative lack of antioxidant defense.[49] Hence, increased mitochondrial production of ROS during chronic hypoxia may be a major factor compromising oligodendrocyte survival. The special vulnerability of newly generated OB neurons to hypoxia could also result from a misbalance between mitochondrial ROS production (increased during hypoxia) and the maturation of the antioxidant defense. The dependence of neuronal and oligodendrocyte survival on a minimum level of O_2 tension gives special significance to the association between angiogenesis and neurogenesis. During hypoxia, newly generated blood vessels could not only help to minimize the effects of O_2 deficiency but might also contribute to paracrine maintenance of stem cells and survival of newly differentiated neurons or glia by means of the release of vascular endothelial trophic factors.[50,51]

Replacement of neurons and myelin-forming oligodendrocytes is essential for normal brain plasticity and repair, and impairment of adult neurogenic centers can lead to neuropsychiatric disorders in humans.[12,52] Therefore, the profound changes induced by chronic hypoxemia in the SVZ and neighboring regions could help explain the neurological symptoms described in chronically hypoxemic patients. Cumulative evidence over the last 30 years has confirmed that cognitive and sensorimotor alterations are frequently seen in COPD patients and that they inversely correlate with arterial pO_2 and with compliance of O_2 therapy.[4,6,7,53] Recent magnetic resonance imaging studies in the brains of COPD patients have shown regional decreases in gray matter density and impairment of white matter microstructural integrity associated with disease severity.[54] Interestingly, a sixfold higher risk of multiple sclerosis, a demyelinating brain disorder, has been reported among individuals (<60 years old) diagnosed with COPD,[55] although this is an isolated observation that needs to be confirmed. Similar to severe COPD, patients who develop chronic mountain sickness due to "de-acclimatization" to high altitude also present well-known neurological disturbances in the form of paresthesias, loss of reflexes, and cognitive impairment.[1,2,10] In this regard, the thinning of capillary walls near a flattened ependyma in the lateral ventricles observed in chronically hypoxic mice might be a fundamental pathophysiological factor in the development of microhemorrhages characteristic of patients presenting high-altitude cerebral edema.[2]

Conclusion

The findings in this report demonstrate that sustained hypoxemia has a profound effect on the structure and function of the brain SVZ neurogenic niche. They provide a solid foundation for further research on the effects of chronic hypoxia on the fate of newly generated cells in the adult brain and their participation in the neurological alterations induced by persistent hypoxemia.

Acknowledgments

This research was supported by the Spanish "Instituto de Salud Carlos III" (XdT, Miguel Servet grant CP12-03217 and PIE13/00004), The Botín Foundation, and The Spanish Ministry of Science and Innovation (Plan Nacional, SAF program). Ricardo Pardal received a Starting Grant from ERC. We would like to thank Margarita Rubio and Rocío Duran for technical assistance. We are grateful to members of the IBIS Animal Facility Core for excellent care of the animals.

Disclosure

The authors report no conflicts of interest in this work.

References

1. Joseph V, Pequignot J-M. Breathing at high altitude. *Cell Mol Life Sci*. 2009;66:3565–3573.
2. Wilson MH, Newman S, Imray CH. The cerebral effects of ascent to high altitudes. *Lancet Neurol*. 2009;8:175–191.
3. Sutherland ER, Cherniack RM. Management of chronic obstructive pulmonary disease. *N Engl J Med*. 2004;350:2689–2697.
4. Schou L, Østergaard B, Rasmussen LS, Rydahl-Hansen S, Phanareth K. Cognitive dysfunction in patients with chronic obstructive pulmonary disease – a systematic review. *Respir Med*. 2012;106:1071–1081.
5. Erecińska M, Silver I. Tissue oxygen tension and brain sensitivity to hypoxia. *Respir Physiol*. 2001;128:263–276.
6. Grant I, Heaton RK, McSweeny JA, Adams KM, Timms RM. Neuropsychologic findings in hypoxemic chronic obstructive pulmonary disease. *Arch Intern Med*. 1982;142:1470–1476.
7. Incalzi RA, Corsonello A, Trojano L, et al. Cognitive training is ineffective in hypoxemic COPD: a six-month randomized controlled trial. *Rejuvenation Res*. 2008;11:239–250.
8. Singh B, Mielke M, Parsaik A, et al. A prospective study of chronic obstructive pulmonary disease and the risk for mild cognitive impairment. *JAMA Neurol*. 2014;71:581–588.
9. Monge C, Arregui A, León-Velarde F. Pathophysiology and epidemiology of chronic mountain sickness. *Int J Sports Med*. 1992;13: S79–S81.
10. Thomas PK, King RH, Feng SF, et al. Neurological manifestations in chronic mountain sickness: the burning feet-burning hands syndrome. *J Neurol Neurosurg Psychiatry*. 2000;69:447–452.
11. Zubieta-Castillo G, Zubieta-Calleja GR, Zubieta-Calleja L. Chronic mountain sickness: the reaction of physical disorders to chronic hypoxia. *J Physiol Pharmacol*. 2006;57(Suppl 4):431–442.
12. Zhao C, Deng W, Gage FH. Mechanisms and functional implications of adult neurogenesis. *Cell*. 2008;132:645–660.
13. Panchision DM. The role of oxygen in regulating neural stem cells in development and disease. *J Cell Physiol*. 2009;220:562–568.
14. Mohyeldin A, Garzón-Muvdi T, Quiñones-Hinojosa A. Oxygen in stem cell biology: a critical component of the stem cell niche. *Cell Stem Cell*. 2010;7:150–161.
15. Suda T, Takubo K, Semenza GL. Metabolic regulation of hematopoietic stem cells in the hypoxic niche. *Cell Stem Cell*. 2011;9:298–310.
16. Platero-Luengo A, González-Granero S, Durán R, et al. An O2-sensitive glomus cell-stem cell synapse induces carotid body growth in chronic hypoxia. *Cell*. 2014;156:291–303.
17. Macías D, Fernández-Agüera MC, Bonilla-Henao V, López-Barneo J. Deletion of the von Hippel-Lindau gene causes sympathoadrenal cell death and impairs chemoreceptor-mediated adaptation to hypoxia. *EMBO Mol Med*. 2014;6:1577–1592.
18. Doetsch F, Caillé I, Lim DA, García-Verdugo JM, Alvarez-Buylla A. Subventricular zone astrocytes are neural stem cells in the adult mammalian brain. *Cell*. 1999;97:703–716.
19. Quiñones-Hinojosa A, Sanai N, Soriano-Navarro M, et al. Cellular composition and cytoarchitecture of the adult human subventricular zone: a niche of neural stem cells. *J Comp Neurol*. 2006;494:415–434.
20. Arvidsson A, Collin T, Kirik D, Kokaia Z, Lindvall O. Neuronal replacement from endogenous precursors in the adult brain after stroke. *Nat Med*. 2002;8:963–970.
21. Picard-Riera N, Decker L, Delarasse C, et al. Experimental autoimmune encephalomyelitis mobilizes neural progenitors from the subventricular zone to undergo oligodendrogenesis in adult mice. *Proc Natl Acad Sci U S A*. 2002;99:13211–13216.
22. Menn B, Garcia-Verdugo JM, Yaschine C, Gonzalez-Perez O, Rowitch D, Alvarez-Buylla A. Origin of oligodendrocytes in the subventricular zone of the adult brain. *J Neurosci*. 2006;26:7907–7918.
23. Gonzalez-Perez O, Romero-Rodriguez R, Soriano-Navarro M, Garcia-Verdugo JM, Alvarez-Buylla A. Epidermal growth factor induces the progeny of subventricular zone type B cells to migrate and differentiate into oligodendrocytes. *Stem Cells*. 2009;27:2032–2043.
24. Martí-Fàbregas J, Romaguera-Ros M, Gómez-Pinedo U, et al. Proliferation in the human ipsilateral subventricular zone after ischemic stroke. *Neurology*. 2010;74:357–365.
25. Capilla-Gonzalez V, Guerrero-Cazares H, Bonsu JM, et al. The subventricular zone is able to respond to a demyelinating lesion after localized radiation. *Stem Cells*. 2014;32:59–69.
26. Pardal R, Ortega-Sáenz P, Durán R, López-Barneo J. Glia-like stem cells sustain physiologic neurogenesis in the adult mammalian carotid body. *Cell*. 2007;131(2):364–377.
27. Ferron SR, Andreu-Agullo C, Mira H, Sanchez P, Marques-Torrejon MA, Farinas I. A combined ex/in vivo assay to detect effects of exogenously added factors in neural stem cells. *Nat Protoc*. 2007;2:849–859.
28. Doetsch F, García-Verdugo JM, Alvarez-Buylla A. Cellular composition and three-dimensional organization of the subventricular germinal zone in the adult mammalian brain. *J Neurosci*. 1997;17: 5046–5061.
29. Johansson CB, Momma S, Clarke DL, Risling M, Lendahl U, Frisén J. Identification of a neural stem cell in the adult mammalian central nervous system. *Cell*. 1999;96:25–34.
30. Brown JP, Couillard-Després S, Cooper-Kuhn CM, Winkler J, Aigner L, Kuhn HG. Transient expression of doublecortin during adult neurogenesis. *J Comp Neurol*. 2003;467:1–10.
31. Luskin MB. Restricted proliferation and migration of postnatally generated neurons derived from the forebrain subventricular zone. *Neuron*. 1993;11:173–189.
32. Lois C, Alvarez-Buylla A. Long-distance neuronal migration in the adult mammalian brain. *Science*. 1994;264:1145–1148.
33. Petreanu L, Alvarez-Buylla A. Maturation and death of adult-born olfactory bulb granule neurons: role of olfaction. *J Neurosci*. 2002;22: 6106–6113.
34. Jin K, Minami M, Lan JQ, et al. Neurogenesis in dentate subgranular zone and rostral subventricular zone after focal cerebral ischemia in the rat. *Proc Natl Acad Sci U S A*. 2001;98:4710–4715.
35. Zhang RL, Zhang ZG, Zhang L, Chopp M. Proliferation and differentiation of progenitor cells in the cortex and the subventricular zone in the adult rat after focal cerebral ischemia. *Neuroscience*. 2001;105: 33–41.
36. Back SA, Han BH, Luo NL, et al. Selective vulnerability of late oligodendrocyte progenitors to hypoxia-ischemia. *J Neurosci*. 2002;22: 455–463.
37. Kako E, Kaneko N, Aoyama M, et al. Subventricular zone-derived oligodendrogenesis in injured neonatal white matter in mice enhanced by a nonerythropoietic erythropoietin derivative. *Stem Cells*. 2012;30: 2234–2247.
38. Oorschot DE, Voss L, Covey MV, et al. Spectrum of short- and long-term brain pathology and long-term behavioral deficits in male repeated hypoxic rats closely resembling human extreme prematurity. *J Neurosci*. 2013;33:11863–11877.
39. Salmaso N, Jablonska B, Scafidi J, Vaccarino FM, Gallo V. Neurobiology of premature brain injury. *Nat Neurosci*. 2014;17:341–346.

40. Ezashi T, Das P, Roberts RM. Low O2 tensions and the prevention of differentiation of hES cells. *Proc Natl Acad Sci U S A*. 2005;102:4783–4788.
41. Yamashita T, Ninomiya M, Hernández Acosta P, et al. Subventricular zone- derived neuroblasts migrate and differentiate into mature neurons in the post-stroke adult striatum. *J Neurosci*. 2006;26:6627–6636.
42. Yang Z, Levison SW. Hypoxia/ischemia expands the regenerative capacity of progenitors in the perinatal subventricular zone. *Neuroscience*. 2006;139:555–564.
43. Zhang ZG, Chopp M. Neurorestorative therapies for stroke: underlying mechanisms and translation to the clinic. *Lancet Neurol*. 2009;8:491–500.
44. Snyder EY, Park KI. Limitations in brain repair. *Nat Med*. 2002;8:928–930.
45. Varela-Nallar L, Rojas-Abalos M, Abbott AC, Moya EA, Iturriaga R, Inestrosa NC. Chronic hypoxia induces the activation of the Wnt/β-catenin signaling pathway and stimulates hippocampal neurogenesis in wild-type and APPswe-PS1ΔE9 transgenic mice in vivo. *Front Cell Neurosci*. 2014;8:17.
46. Morrison SJ, Csete M, Groves AK, Melega W, Wold B, Anderson DJ. Culture in reduced levels of oxygen promotes clonogenic sympathoadrenal differentiation by isolated neural crest stem cells. *J Neurosci*. 2000;20:7370–7376.
47. Studer L, Csete M, Lee SH, et al. Enhanced proliferation, survival, and dopaminergic differentiation of CNS precursors in lowered oxygen. *J Neurosci*. 2000;20:7377–7383.
48. Bradl M, Lassmann H. Oligodendrocytes: biology and pathology. *Acta Neuropathol*. 2010;119:37–53.
49. Thorburne S, Juurlink B. Low glutathione and high iron govern the susceptibility of oligodendroglial precursors to oxidative stress. *J Neurochem*. 1996;67:1014–1022.
50. Shen Q, Goderie SK, Jin L, et al. Endothelial cells stimulate self-renewal and expand neurogenesis of neural stem cells. *Science*. 2004;304:1338–1340.
51. Porlan E, Perez-Villalba A, Delgado AC, Ferrón SR. Paracrine regulation of neural stem cells in the subependymal zone. *Arch Biochem Biophys*. 2013;534:11–19.
52. Ming G-L, Song H. Adult neurogenesis in the mammalian brain: significant answers and significant questions. *Neuron*. 2011;70:687–702.
53. De Carolis A, Giubilei F, Caselli G, et al. Chronic obstructive pulmonary disease is associated with altered neuropsychological performance in young adults. *Dement Geriatr Cogn Dis Extra*. 2011;1:402–408.
54. Zhang H, Wang X, Lin J, et al. Grey and white matter abnormalities in chronic obstructive pulmonary disease: a case-control study. *BMJ Open*. 2012;2(2):e000844.
55. Egesten A, Brandt L, Olsson T, et al. Increased prevalence of multiple sclerosis among COPD patients and their first-degree relatives: a population-based study. *Lung*. 2008;186:173–178.

Supplementary materials

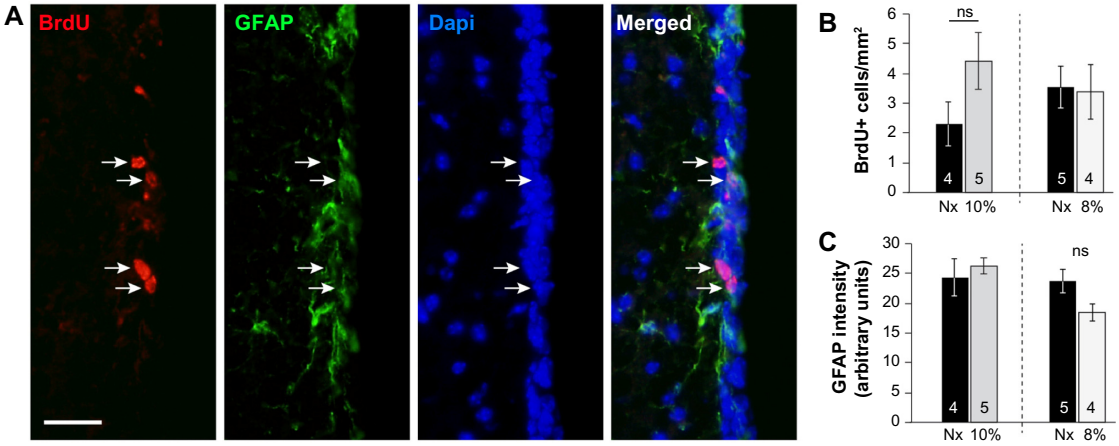

Figure S1 Proliferation and number of neural stem cells in the SVZ is not affected by hypoxia.

Notes: (**A**) Immunohistochemical detection of BrdU (red, arrows) and GFAP (green) in the lateral ventricle wall of a mouse maintained in normoxia (21% O_2 tension) 11 days after three injections of BrdU. Dapi stains nuclei (blue). (**B**) Mean number ± SEM of BrdU cells in the lateral wall of the lateral ventricle, from animals maintained in normoxia (Nx) or in hypoxia (10% or 8% O_2). $P>0.05$. (**C**) Mean intensity ± SEM of GFAP staining measured in the 30 μm width from the lateral border of the ventricle in normoxic (Nx) or hypoxic (either 10% or 8% O_2) animals. The number of individuals is shown at the bottom of each vertical bar. Scale bar =30 μm.

Abbreviations: SVZ, subventricular zone; BrdU, 5-bromo-2′-deoxyuridine; GFAP, glial fibrillary acidic protein; Dapi, 4′,6-diamidino-2-phenylindole dihydrochloride; SEM, standard error of the mean; ns, not significant.

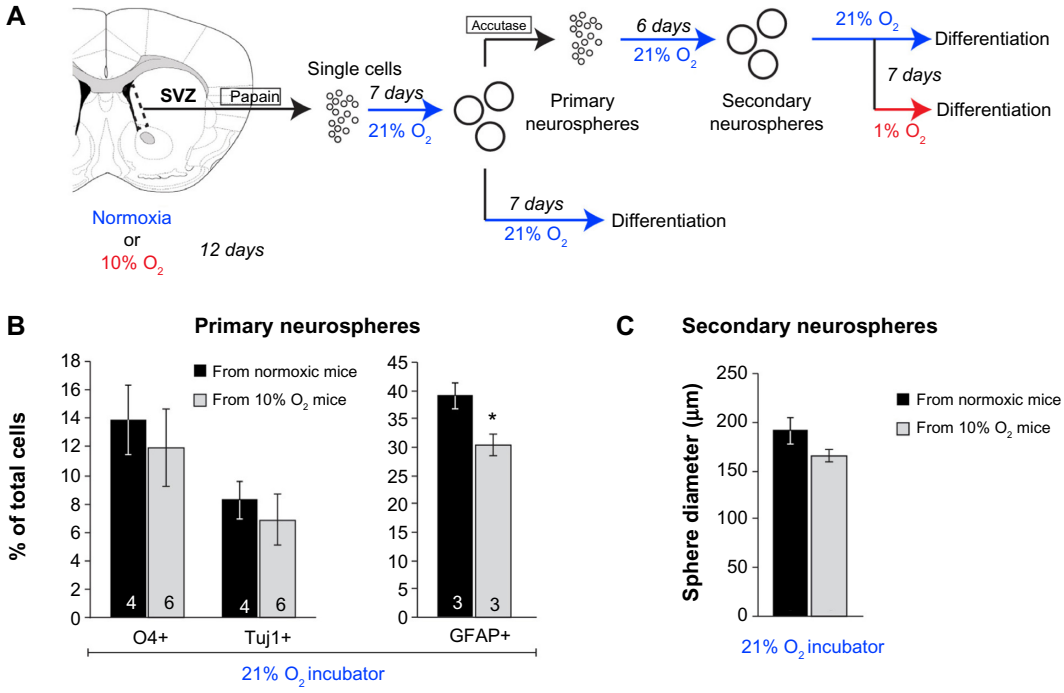

Figure S2 (*Continued*)

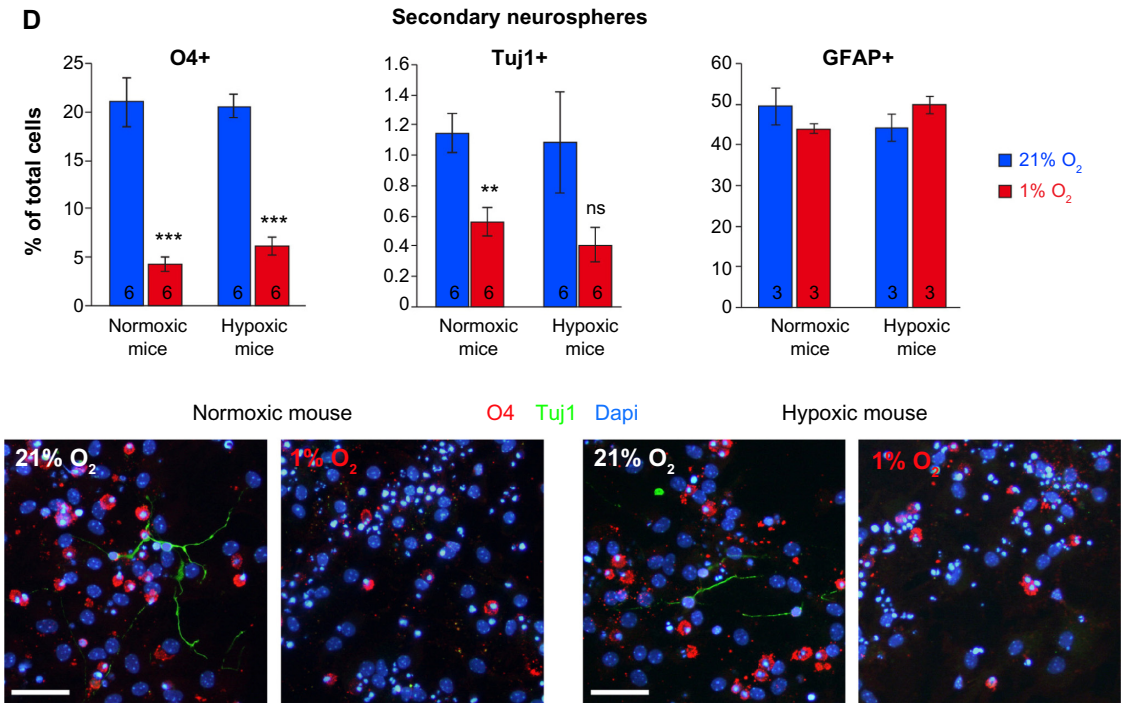

Figure S2 In vitro SVZ secondary neurospheres formation and differentiation.

Notes: (**A**) Schematic diagram depicting the experimental design. Single-cell suspension was obtained by papain digestion of SVZ tissue dissected from mice maintained either in normoxia (21% O_2) or in hypoxia (10% O_2) for 12 days. Primary neurospheres were obtained after 7 days and either placed in differentiation medium for 7 days in 21% O_2 atmosphere, or dissociated by accutase digestion to obtain single cells that were placed in neurosphere culture conditions for 6 days. Secondary neurospheres were then placed in differentiation conditions for 7 days in 21% or 1% O_2 atmosphere. (**B**) Bargraphs indicate the percentage (± SEM) of oligodendrocytes (O4+), neurons (Tuj1+), and astrocytes (GFAP+) in primary neurospheres from animals maintained in normoxia or hypoxia after 7 days of differentiation at 21% O_2 atmosphere. (**C**) Mean diameter (± SEM) of secondary SVZ neurospheres obtained from normoxic or hypoxic (10% O_2) animals cultured at 21% O_2 for 7 days. The data indicate that self-renewal of progenitors derived from hypoxic mice is not impaired. (**D**) Bargraphs indicate the percentage (± SEM) of O4+, Tuj1+, and GFAP+ cells in secondary neurospheres derived from normoxic or hypoxic (10% O_2) mice and differentiated for 7 days in 21% or 1% O_2. A selective decrease in oligodendrocytic and neuronal population occurred at 1% O_2 in comparison to 21% O_2 atmosphere regardless of the previous normoxic or hypoxic status of the mice. The number of GFAP+ cells (astrocytes) remained unchanged. Microphotographs (bottom panel) illustrate the loss of O4+ (red) and Tuj1+ (green) in 1% O_2 in both normoxic and hypoxic mice-derived secondary neurospheres. Nuclei are stained in blue. Scale bar =50 µm. The number of individuals per condition is indicated at the bottom of each vertical bar. *$P<0.05$, **$P<0.01$, and ***$P<0.001$.

Abbreviations: SVZ, subventricular zone; SEM, standard error of the mean; GFAP, glial fibrillary acidic protein; ns, not significant; Dapi, 4′,6-diamidino-2-phenylindole dihydrochloride.

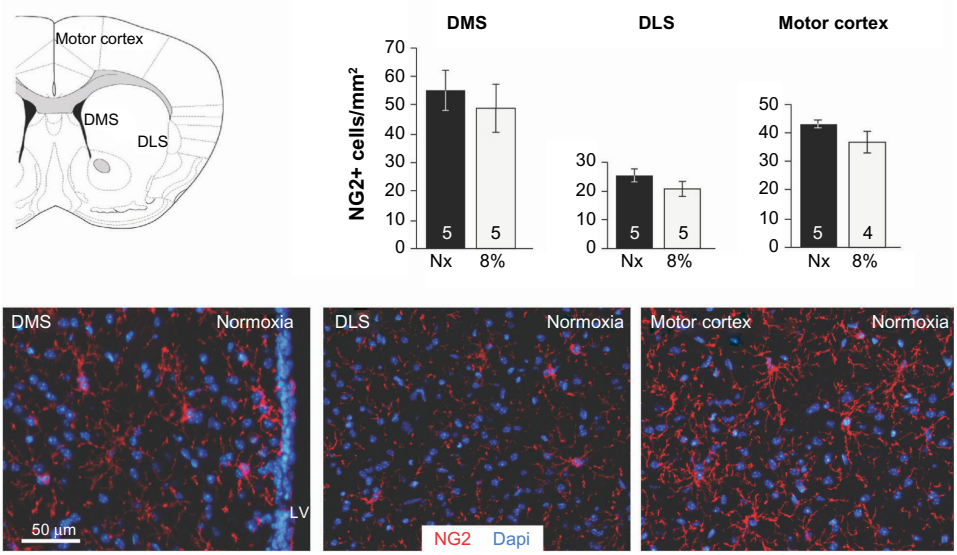

Figure S3 Immature oligodendrocyte progenitors are not affected by hypoxia.

Notes: Immature oligodendrocyte progenitors (NG2+) were quantified in the DMS, DLS, and motor cortex as depicted in the mouse brain diagram (top left). Bargraphs show that the number (± SEM) of NG2+ cells per mm^2 in the DMS, DLS, and motor cortex is not affected after 12 days in 8% hypoxia. The number of individuals is shown at the bottom of each vertical bar. Coronal sections in normoxic animals illustrate the NG2 (red) staining with Dapi-stained nuclei (blue) in the three regions analyzed. Scale bar =50 µm. Note that the DMS results are also presented in the main manuscript.

Abbreviations: DLS, dorsolateral striatum; DMS, dorsomedial striatum; SEM, standard error of the mean; Dapi, 4′,6-diamidino-2-phenylindole dihydrochloride; LV, lateral ventricle.

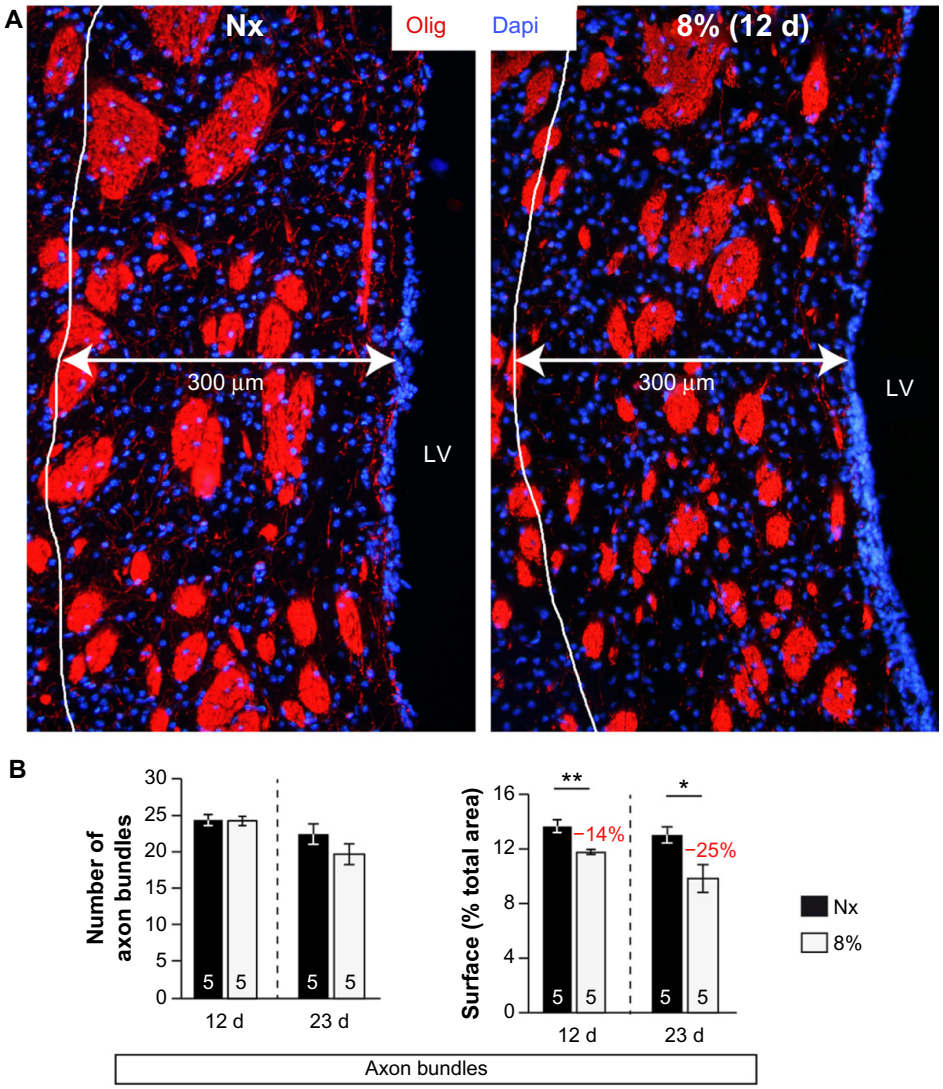

Figure S4 Axon bundles reduced size in chronic hypoxia.
Notes: (**A**) Coronal sections showing Olig+ (red) and Dapi+ (blue) staining in the SVZ, and the neighboring striatum, in normoxic (Nx) and hypoxic animals. The double arrowhead, 300 µm from the LV, indicates the striatal region analyzed. The low-magnification photographs illustrate the slightly thinner Olig-stained striatal bundles in animals maintained at 8% hypoxia for 12 days versus normoxic animals. (**B**) Vertical bargraphs indicate the average number (left) and size (right) of the striatal axon bundles. Values in red indicate the percentage of decrease from the normoxic counterparts. *$P<0.05$ and **$P<0.01$.
Abbreviations: Dapi, 4′,6-diamidino-2-phenylindole dihydrochloride; SVZ, subventricular zone; LV, lateral ventricle.

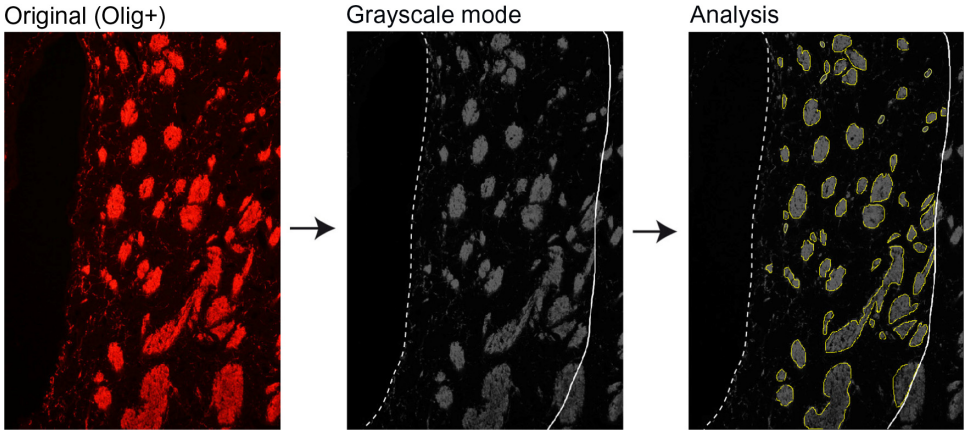

Figure S5 Estimation of striatal fiber bundle density.
Notes: The original image (left) was converted to grayscale mode for binary image processing (middle), and the limit for the 300 µm (plotted line) was set from the ventricle's wall (plain line). Axon bundles contour were drawn (yellow lines) for surface area and intra-bundle Olig density analysis using Image J software.

Extended materials and methods

Antibodies and special reagents

The specificity of each antibody used in this study has been extensively tested by other groups and showed specific and expected staining in our hands. Primary antibodies were used as follows: anti-5-bromo-2′-deoxyuridine (BrdU, clone BU1/75 [ICR1] ab6326 from Abcam), 1:200; anti-proliferating cell nuclear antigen (PCNA, clone PC10, M0879, Dako), 1:1,000; anti-neuronal nuclei (NeuN, clone A60, MAB377 Millipore), 1:1,000; anti-glial fibrillary acidic protein (GFAP, Z0334, Dako), 1:1,000; anti-doublecortin (DCX, sc-8066, Santa Cruz Biotechnology), 1:500; anti-oligodendrocytes, also known as RIP (Olig, MAB1580, Millipore), 1:1,000; anti-chondroitin sulfate proteoglycan (NG2, AB5320, Millipore), 1:100; anti-oligodendrocyte marker O4 (clone 81, MAB345, Millipore), 1:500; anti-beta III tubulin (Tuj1, ab18207, Abcam), 1:500. We used secondary antibodies anti-mouse IgG or IgM, anti-rabbit IgG, anti-goat IgG, or anti-rat IgG conjugated with Alexa Fluor 488 or Alexa Fluor 568 (1:500) (Invitrogen). Mouse on mouse M.O.M. kit (BMK-2202, Vector Laboratories). Apoptotic cells were revealed using a Click-iT® TUNEL Alexa Fluor® Imaging Assay (C10245, Invitrogen). Nuclei were stained with 4′,6-diamidino-2-phenylindole dihydrochloride (Dapi, D9542, Sigma). The thymidine analog BrdU (B5002, Sigma) was prepared in sterile saline and dissolved by sonication just prior injection. Trypsin inhibitor solution contains 2.5 mg/mL trypsin inhibitor (T9253, Sigma), 2.5 mg/mL bovine serum albumin (A8022, Sigma), 4.5 mg/mL D-(+)-glucose (G7021, Sigma), and 26 mM $NaHCO_3$ in Earle's balanced salt solution (24010, Gibco).

Immunohistochemistry and immunocytofluorescence

Mice were intracardially perfused with 0.1 M phosphate-buffered saline (PBS) followed by 4% paraformaldehyde in PBS pH 7.4. Following a 1-hour postfixation step, brains were washed in PBS 0.1 M, cryoprotected in PBS with 30% sucrose, embedded in Tissue-Tek® O.C.T. Compound, and frozen on dry ice. Using a cryostat (CM 1950, Leica, Germany), 10 µm coronal cryosections were obtained in ten series on Superfrost plus slides (Thermo Scientific). Each series containing 8–9 sections was spaced 200 µm approximately ranging from +1.10 mm to –0.50 mm from bregma in anteroposterior coordinates. For each immunoassay, one complete series (ie, one slide) was used per animal. Sections were stored at –20°C until use. After being brought back at room temperature (RT), cryosections were rehydrated in PBS. Some primary antibodies required specific pretreatment: to uncover BrdU and PCNA, we used a solution of sodium citrate 10 mM, pH 6 with 0.05% Tween-20 at 95°C for 20 minutes. For PCNA and Olig detection, a 1-hour pretreatment with M.O.M. prevents background staining. Sections were then washed with PBS and incubated for 1 hour at RT in a blocking solution (PBS 0.1 M with bovine serum albumin 1 mg/mL, 10% fetal bovine serum, and 0.1% Triton X-100). Then, sections were incubated with primary antibodies diluted in the aforementioned blocking solution overnight at 4°C. Sections were extensively washed in PBS with 0.1% Triton X-100, and incubated with the appropriate secondary Alexa 488- or Alexa 568-conjugated antibodies in blocking buffer for 1 hour at RT. Dapi 0.5 µg/mL was added in the last wash for nuclear staining. Slides were coverslipped with Fluoro-gel (17985-11, EMS, Hatfield, PA, USA). Fluorescence images were obtained with a BX61 microscope equipped with a DP70 camera (Olympus). Given the inter-experimental groups difference that may occur, only animals from the same batch were analyzed side by side. Thus, 10% hypoxia animals were compared with their normoxic littermates, and 8% hypoxia mice were compared with their normoxic littermates. Photos were acquired at a 4,080×3,072 pixels resolution under the aforementioned fluorescent microscope with same exposure and contrast settings between different conditions in a given staining. Alexa 488-labeled cells were detected with the U-MWIBA2 filter (EX530-550/DM570/EM590, Olympus). Alexa 568-labeled cells were examined with the U-N41021 filter (EX550-580/DM585/EM620). Dapi-labeled nuclei were observed with the U-MNU2 filter (EX360-370/DM400/EM420). An experimenter blinded to the treatment protocol performed all photos acquisition, processing, and cell quantifications. For BrdU and PCNA analysis in the subventricular zone (SVZ), 10–14 photos of the SVZ for each staining and Dapi were acquired per animal with the objective ×20. Images were processed with Photoshop CS5 (Adobe) to merge BrdU or PCNA staining with Dapi-positive nuclei. Only dual-labeled nuclei that were lying along the wall of the lateral ventricle were considered. Results were expressed as the average number of BrdU or PCNA-positive cells ± standard error of the mean (SEM) per SVZ mm.

For DCX analysis in the SVZ, 8–12 photos of the DCX staining in the lateral wall of the SVZ were acquired. Analysis was undertaken by converting color images to 8-bit grayscale mode, and by measuring both the intensity and the surface area of the region of interest using Image J 1.46r software (NIH), and then multiplying the intensity by area values. This method provides a solid estimation (in arbitrary units) of the population of DCX-positive cells in each SVZ photos.

For BrdU and GFAP analysis in the SVZ of animals sacrificed 11 days after BrdU injection (Figure S1), 9–13 photos of the SVZ for each staining plus Dapi were acquired per animal with ×20 objective. Only dual-labeled BrdU+/Dapi+ nuclei that were lying along the wall of the lateral ventricle were considered. The GFAP intensity was measured in the SVZ area corresponding to a 30 µm band from the limit of the ventricular lumen. Color images were converted to 8-bit mode and were quantified using Image J. Results were expressed as the mean of the intensity ± SEM in arbitrary unit.

For Olig analysis in the dorsomedial striatum (DMS), 8–12 photos per animal were acquired for Olig and Dapi staining in the DMS, within a limit of 300 µm from the lateral ventricle wall. Since Olig is a cytoplasmic marker, only dual-labeled Dapi/Olig cells were considered as immunoreactive, and results are expressed as the average number of Olig-positive cells ± SEM per mm^2. To estimate the levels of myelin, Olig staining images were converted to grayscale to determine the axon bundles size and the optical density (binary image processing of black and white) inside the axon bundles and between them (inter-bundles space) (Figure S5 is an example). Values for each animal were used to determine mean counts, and these were used to generate mean ± SEM values for each group. Immature oligodendrocytes were detected with NG2/Dapi staining and quantified within the same limits as for Olig staining.

For BrdU-positive cells migration to the olfactory bulb (OB), mice were sacrificed 11 days after 3× BrdU 50 mg/kg injections, and OB was removed and examined. BrdU and Dapi staining was performed as described earlier. TUNEL/NeuN staining was performed following the manufacturer instructions with minor modifications. Intestine sections from the same mice were used as a control for positive TUNEL staining, since apoptosis is observed at the surface of the gastric pits.[1] TUNEL- or BrdU-positive cells were counted in the granular cell layer in six to ten photos per animal that were acquired with a ×20 objective. Values are expressed as mean ± SEM positive cells per mm^2 for each group. The percent of neuronal (NeuN positive) cells over the total cells in the OB was quantified in the same photos as those used for TUNEL quantification. Dapi+ nuclei displaying a moon-like shape were not taken into the total nuclei counting but were considered as endothelial cells and counted as such.

For secondary neurosphere differentiation assay and immunocytochemistry, glass coverslips in 24-well plates were treated, prior to plating, with 0.5 mg/mL human fibronectin (Biomedical Technologies) for adherence. Neurospheres (6 days old) derived from primary neurospheres generated from normoxic or hypoxic (10% O_2 tension) animals were plated in the mitogen-free medium as described in the main manuscript and placed in 5% CO_2 incubators with 21% or 1% O_2 levels. After 7 days in differentiation conditions, cells were fixed and treated for immunocytochemistry as described in the "Materials and methods" section. Two photos per condition were used for analysis of the following staining: O4, Tuj1, and GFAP. The percentage of O4+, Tuj1+, and GFAP+ cells was calculated over the total number of Dapi+ nuclei.

Reference

1. Frisch SM, Francis H. Disruption of epithelial cell-matrix interactions induces apoptosis. *J Cell Biol*. 1994;124:619–626.

Hypoxia

Dovepress

Publish your work in this journal

Hypoxia is an international, peer-reviewed, open access journal that aims to improve understanding of the biological response to hypoxia. The journal will publish original research articles, reviews, methodological advances, clinical studies, and expert opinions that identify developments in the regulation of the physiological and pathological responses to hypoxia and in the therapeutic targeting of hypoxia-responsive pathways. The manuscript management system is completely online and includes a very quick and fair peer-review system, which is all easy to use. Visit http://www.dovepress.com/testimonials.php to read real quotes from published authors.

Submit your manuscript here: http://www.dovepress.com/hypoxia-journal